

# Quantum tele-amplification with a continuous variable superposition state

Jonas S. Neergaard-Nielsen,<sup>1,2</sup> Yujiro Eto,<sup>1,3</sup> Chang-Woo Lee,<sup>4,5</sup> Hyunseok Jeong,<sup>4,6</sup> and Masahide Sasaki<sup>1</sup>

<sup>1</sup> *National Institute of Information and Communications Technology (NICT),  
4-2-1 Nukui-kitamachi, Koganei, Tokyo 184-8795, Japan*

<sup>2</sup> *Department of Physics, Technical University of Denmark, Fysikvej, 2800 Kgs. Lyngby, Denmark*

<sup>3</sup> *Department of Physics, Gakushuin University, 1-5-1 Mejiro, Toshima-ku, Tokyo 171-8588, Japan*

<sup>4</sup> *Center for Macroscopic Quantum Control, Department of Physics and Astronomy,  
Seoul National University, Seoul, 151-747, Korea*

<sup>5</sup> *Department of Physics, Texas A&M University at Qatar, PO Box 23874, Doha, Qatar*

<sup>6</sup> *Centre for Quantum Computation and Communication Technology, School of  
Mathematics and Physics, University of Queensland, Brisbane, Queensland 4072, Australia*

(Dated: March 7, 2013)

**Optical coherent states are classical light fields with high purity, and are essential carriers of information in optical networks. If these states could be controlled in the quantum regime, allowing for their quantum superposition (referred to as a Schrödinger cat state), then novel quantum-enhanced functions such as coherent-state quantum computing (CSQC)<sup>1–5</sup>, quantum metrology<sup>6,7</sup>, and a quantum repeater<sup>8,9</sup>, could be realized in the networks. Optical cat states are now routinely generated in the laboratories. An important next challenge is to use them for implementing the aforementioned functions. Here we demonstrate a basic CSQC protocol, where a cat state is used as an entanglement resource for teleporting a coherent state with an amplitude gain. We also show how this can be extended to a loss-tolerant quantum relay of multi-ary phase-shift keyed coherent states. These protocols could be useful both in optical and quantum communications.**

Among various optical implementations of quantum information processing (QIP), coherent-state quantum computing (CSQC) is of special interest for enhancing the performance of optical communications, where information is encoded into coherent states. These are the only states that can be transmitted preserving the state purity even through a lossy channel since they are eigenstates of the annihilation operator,  $\hat{a}|\alpha\rangle = \alpha|\alpha\rangle$ . Hence, a simple classical encoding with coherent states can be the optimal strategy of the transmitter to achieve the ultimate capacity of a lossy optical channel<sup>10</sup>. On the receiver side, the sequence of coherent-state pulses should be decoded fully quantum mechanically by employing a collective measurement with CSQC<sup>11</sup>. This scheme can realize communication with larger capacity, beating the conventional homodyne limit of optical communications<sup>12</sup>. Although practical implementation of CSQC remains a big challenge, recent progress in generating<sup>13–17</sup> and manipulating<sup>18,19</sup> optical cat states makes it realistic to implement its basic building blocks. In this paper, we propose and demonstrate the first operational application of cat states for QIP, where a cat

state is used as the entanglement resource for teleporting a coherent state with an amplitude gain. We also propose its new application to quantum key distribution (QKD), namely a loss-tolerant quantum relay of multi-ary phase-shift keyed (M-PSK) coherent states that does not assume a trusted node. We present its proof-of-principle demonstration with binary PSK states.

The basic scheme of teleportation from Alice to Bob of a cat state qubit  $|\psi\rangle_A = c_+|\alpha\rangle_A + c_-|-\alpha\rangle_A$ , which is a variation of the schemes in refs. 20 and 21, is depicted in Fig. 1a. Bob prepares an odd cat state  $|\Phi_-(\beta)\rangle_B = \mathcal{N}_-(|\beta\rangle_B - |-\beta\rangle_B)$  with normalization  $\mathcal{N}_-$  and splits it into an entangled cat state over paths B and C via a beam-splitter (BS)  $\hat{V}_{BC}$  with reflectivity  $R_B$ . He sends one part of it to Alice at port C. She then combines it on an  $R_A$ -reflectivity BS with her input  $|\psi\rangle_A$  at port A as

$$|\Psi\rangle_{ABC} = \hat{V}_{AC}|\psi\rangle_A \hat{V}_{BC}|\Phi_-\rangle_B |0\rangle_C. \quad (1)$$

She finally measures modes A and C by single-photon detectors. By conditioning port B on her measurement result, Bob can restore Alice's input.

The amplitude of the resource cat state is set as  $\beta = \alpha\sqrt{(1-R_A)/R_AR_B}$ , such that the components at port A turn into either the vacuum or a non-vacuum state. Then, when Alice's detectors register a single photon at port A and nothing at port C – denoted (1,0) – Bob unambiguously obtains the state (Supplementary Information)

$$AC\langle 1,0|\Psi\rangle_{ABC} \propto c_+|-g\alpha\rangle_B + c_-|g\alpha\rangle_B, \quad (2)$$

where  $g = \sqrt{(1-R_A)(1-R_B)/R_AR_B}$  is the gain parameter. By a simple  $\pi$ -phase shift, it can be transformed to Alice's input  $|\psi\rangle_A$ , but with a modified amplitude  $\alpha' = g\alpha$ . This process, previously suggested in ref. 3, we will call *tele-amplification*.

Unfortunately this tele-amplification is vulnerable to losses. Suppose the channel between Alice and Bob is subject to a linear loss  $R_E$ . The amplitude of the resource cat state should then be chosen as

$$\beta = \sqrt{\frac{1-R_A}{R_AR_B(1-R_E)}}\alpha. \quad (3)$$

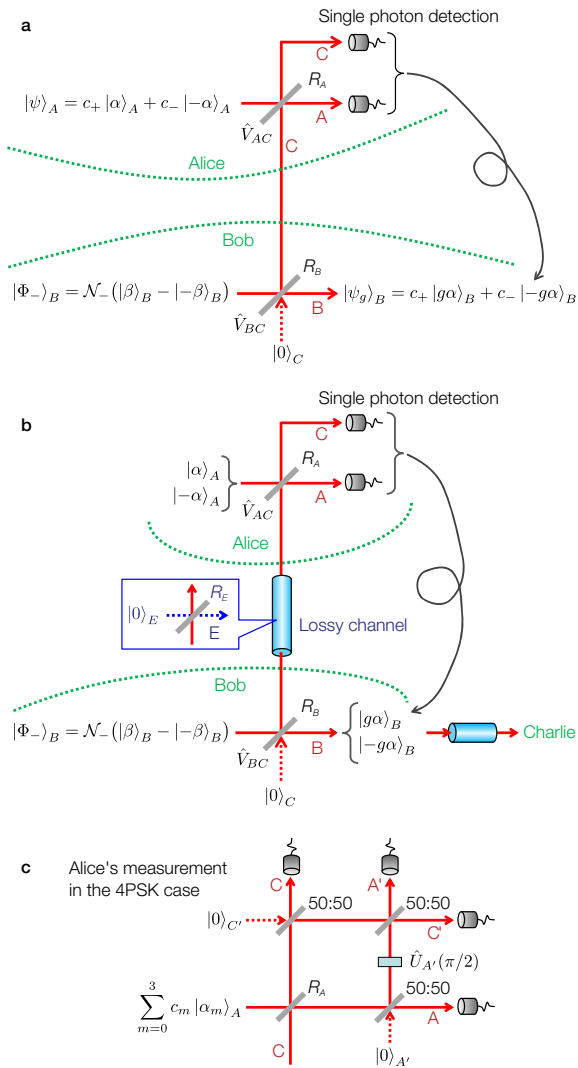


FIG. 1: Scheme of quantum tele-amplification and quantum relay. **a** Tele-amplification of binary cat-state in an ideal lossless channel.  $R_A$  and  $R_B$  are the reflectivities of the BSs. **b** Loss tolerant quantum relay.  $R_E$  is the reflectivity of the BS which models the lossy channel. **c** Alice's four-port measurement for the case of 4PSK states.

After conditioning on Alice's detection event  $(1,0)$ , Bob's state gets entangled with an external mode  $E$  as

$$|\psi\rangle_A |0\rangle_E \mapsto c_+ |-g\alpha\rangle_B |\varepsilon\rangle_E + c_- |g\alpha\rangle_B |-\varepsilon\rangle_E \quad (4)$$

with the modified gain including the loss rate  $R_E$

$$g = \sqrt{\frac{(1-R_A)(1-R_B)}{R_A R_B (1-R_E)}}. \quad (5)$$

Here  $\varepsilon = \sqrt{(1-R_A)R_E/R_A(1-R_E)}\alpha$ . Thus, the output at Bob is generally in a decohered state.

One can, however, see that if Alice's inputs are restricted to classical components,  $|\alpha\rangle$  or  $|\alpha\rangle$ , as in Fig. 1b, the output state can be completely disentangled from

the external mode. This means that the coherent states can be tele-amplified faithfully to the target states even through the lossy channel as

$$|\pm\alpha\rangle_A \mapsto |\pm g\alpha\rangle_B. \quad (6)$$

This is referred to as *loss-tolerant quantum relay*. In this context, Bob plays the role of an intermediate node, restores the target states  $|\pm g\alpha\rangle_B$ , and sends them to the terminal node, Charlie.

This simplest binary case can be extended into M-PSK coherent states. Let us show it for the 4-PSK case,  $|\alpha_m\rangle$ , ( $\alpha_m = i^m \alpha$ ,  $m = 0, 1, 2, 3$ ). Bob should prepare a 4-component cat state

$$|\Phi\rangle_B = \mathcal{N} \sum_{k=0}^3 i^k |i^k \beta\rangle_B \quad (7)$$

as a resource. This state is beam-split, and is shared with Alice. We set  $R_A = 0.5$ . As in Fig. 1c, Alice performs a four-port single-photon detection at paths A, A', C, and C' on this state. Depending on the set of results at the four ports, (A, A', C, C'), the inputs are tele-amplified as

$$\begin{aligned} |\alpha_m\rangle &\mapsto |g\alpha_m\rangle, & \text{for } (0, 1, 1, 1), \\ |\alpha_m\rangle &\mapsto |ig\alpha_m\rangle, & \text{for } (1, 0, 1, 1), \\ |\alpha_m\rangle &\mapsto |-g\alpha_m\rangle, & \text{for } (1, 1, 0, 1), \\ |\alpha_m\rangle &\mapsto |-ig\alpha_m\rangle, & \text{for } (1, 1, 1, 0). \end{aligned} \quad (8)$$

Thus, the simple tele-amplification is performed for the result  $(0,1,1,1)$ . Moreover the output state can be switched to another element by choosing an appropriate click pattern at Alice (Supplementary Information).

The faithful relay itself can also be realized in a classical way, where Bob at the intermediate node performs an unambiguous state discrimination on the signal state, reproduces an amplified state for his confident result, and finally resends it to Charlie. This classical relay cannot, however, be applied to a QKD relay node without the trusted node assumption. In contrast, a quantum relay can be carried out in the fully quantum domain, without Bob's knowing the signal state itself, though at the expense of preparing the entangled cat state, and an appropriate entanglement verification session. Similar ideas for single-photon QKD were presented in refs. 22 and 23.

Our loss-tolerant quantum relay is particularly useful for extending the distance of QKD which uses PSK coherent states, such as B92 and BB84<sup>24-26</sup>. Although the secure key generation probabilities at short distances slightly degrades from the original PSK-BB84, they can remain at reasonable levels up to much longer distances by the loss-tolerant quantum relay (Supplementary Information).

We carried out an experimental demonstration of the tele-amplification in the simplest case of binary PSK as in Fig. 1b to realize Eq. (6). The resource cat state  $|\Phi\rangle_B$  was generated by photon-subtraction from a squeezed

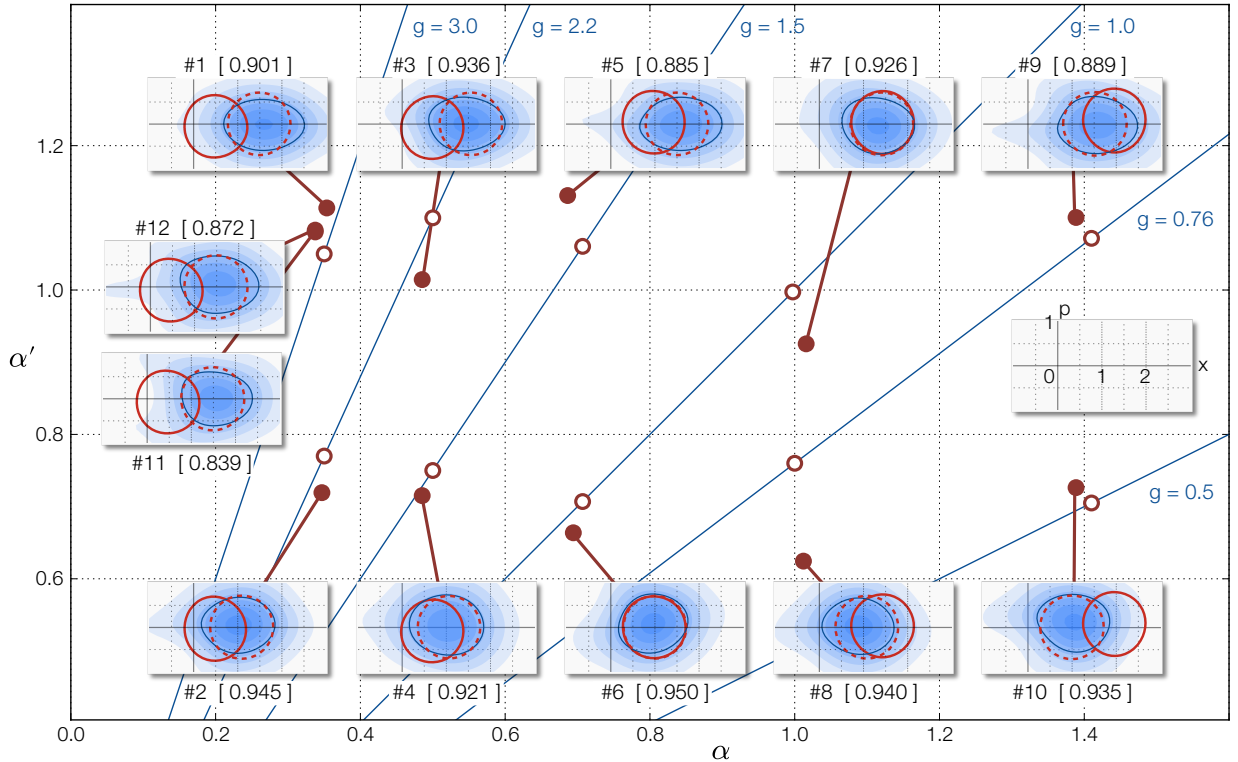


FIG. 2: Measured results for the twelve cases. The blue straight lines represent  $\alpha' = g\alpha$ . The open circles represent the sets of  $\alpha$  and  $g_{tg}$  in Table I. The fidelities between the measured states and the targeted  $|g_{tg}\alpha\rangle$  are indicated by the numbers in brackets. Filled circles represent the amplitudes  $\alpha$  ( $\alpha'$ ) of the coherent states that have the maximum fidelity with the measured input (output) states. **Insets:** Output state Wigner functions are shown in blue contour plots. The red solid and dashed circles are for the input and ideal targeted states, respectively.

vacuum with anti-squeezing along the real axis in phase space (Methods). Bob's BS was set to  $R_B = 0.1$ . For a given desired gain  $g$ , we varied  $R_A$  according to Eq. (5). The resource cat-state amplitude  $\beta$ , experimentally tuned by the squeezing level, was then set by Eq. (3). The detector at port C was omitted with negligible effect on the outcomes since the events  $(A,C)=(1,1)$  would be rare. Bob's output state was characterized by homodyne tomography.

We tested twelve settings as summarized in Table I. The five different input amplitudes  $\alpha$  were real and ranged between 0.35 and 1.4. The protocol was carried out only for  $|\alpha\rangle$  because the outcome for  $|\alpha\rangle$  would be trivially identical. The measured results are shown in Fig. 2. The blue straight lines are gain curves  $\alpha' = g\alpha$  in the  $(\alpha, \alpha')$  diagram. The open circles plotted along these lines represent sets of  $\alpha$  and  $g_{tg}$  in Table I. The Wigner functions of the tomographically reconstructed tele-amplified output states  $\hat{\rho}_{out}$  are shown as blue contour plots in the insets. One contour level is highlighted for comparison with the targeted states  $|g_{tg}\alpha\rangle$  (red dashed) and the actual input states  $\hat{\rho}_{in} \approx |\alpha\rangle\langle\alpha|$  (red solid, also characterized by homodyne tomography). The discrepancies between  $\hat{\rho}_{out}$  and  $|g_{tg}\alpha\rangle$  are due to imperfections, including the deviation of the photon-subtracted

state from the ideal resource cat, losses, impurity, and Alice's use of an on/off detector instead of two single-photon detectors. For each setting, we calculate which coherent states  $|\alpha\rangle, |\alpha'\rangle$  have the highest fidelity with the measured input and output states, respectively, that is,  $\alpha = \text{argmax}_{\gamma} \langle\gamma|\hat{\rho}_{in}|\gamma\rangle$  and  $\alpha' = \text{argmax}_{\gamma'} \langle\gamma'|\hat{\rho}_{out}|\gamma'\rangle$ . These  $(\alpha, \alpha')$  pairs are marked as filled circles.

Despite the imperfections, the tele-amplification succeeded with high fidelities  $\mathcal{F} = \langle g_{tg}\alpha|\hat{\rho}_{out}|g_{tg}\alpha\rangle$  between 0.89 and 0.95 as shown next to each inset. The obtained amplitudes (filled circles) are close to the targeted ones (open circles) in almost all cases. The success probabilities were in the range 0.3% to 0.65% (Methods). For larger  $\alpha'$ , the Wigner function shapes are slightly elongated due to the larger squeezing needed to produce those states. We note that our experimental settings were not fully optimized by taking into account spectral mode mismatch between the resource cat and input coherent states as well as between the APD and homodyne detectors. Had we done it, we estimate the achieved fidelities to have been 0.94–0.99.

The settings #11 and 12 had an additional 80% loss ( $R_E = 0.8$ ) in the channel from Bob to Alice. In #11,  $R_A = 0.5$  for the original lossless setting (as in #1), while in #12,  $R_A = 0.83$  as optimized according to Eq. (5), re-

#	$\alpha$	$g_{\text{tg}}$	$\beta$	$R_A$	$R_E$	$\mathcal{F}$
1	0.35	3.0	1.11	0.50	0	0.901
2	0.35	2.2	0.81	0.65	0	0.945
3	0.50	2.2	1.16	0.65	0	0.936
4	0.50	1.5	0.79	0.80	0	0.921
5	0.71	1.5	1.12	0.80	0	0.885
6	0.71	1.0	0.75	0.90	0	0.950
7	1.00	1.0	1.05	0.90	0	0.926
8	1.00	0.76	0.80	0.94	0	0.940
9	1.41	0.76	1.13	0.94	0	0.889
10	1.41	0.50	0.74	0.97	0	0.935
11	0.35	3.0	1.11	0.50	0.8	0.839
12	0.35	3.0	1.11	0.83	0.8	0.872

TABLE I: Desired tele-amplification for the twelve settings of input coherent states and gains.  $g_{\text{tg}}$  is the targeted gain. The last column shows the obtained teleportation fidelities.

sulting in success probabilities of 0.17% and 0.11%. The fidelities with the target state are as high as 0.839 and 0.872, respectively, as compared with 0.901 in the lossless case. This demonstrates the loss tolerance of the protocol.

Teleportation of a cat-state qubit as in Eqs. (1-2) is a prerequisite for CSQC. Interestingly, the tele-amplification allows to convert between different amplitude qubit bases. Although we previously generated such arbitrary cat qubits<sup>18,27</sup>, it was not feasible to tele-amplify them with the current setup since three simultaneous APD clicks would be needed. Instead we simulated this protocol by accurately modelling the current experiment including all relevant practical imperfections (Supplementary Information). Figure 3 shows the average fidelities between the teleported state for an input cat-state qubit and an output state from the model (Methods). For a wide range of input amplitudes  $\alpha$  and output amplitudes  $\alpha'$ , it is possible to surpass the classical limit of  $2/3$ .

Finally we make a brief comparison between our scheme and the quantum noiseless amplifier with single-photon ancilla<sup>28-30</sup>. The latter is intended to noiselessly amplify a coherent state with an unknown amplitude at the cost of the success probability. In contrast, our scheme assumes the known amplitude  $\alpha$  but instead enables one to tele-amplify PSK coherent states over a lossy channel with perfect fidelity and high success probability. It can also implement, in principle, the teleportation of their arbitrary superpositions.

In summary, we presented tele-amplification and loss-tolerant quantum relay of coherent states as the first operational application of optical cat states. The scheme is an essential building block for CSQC as well as quantum communications.

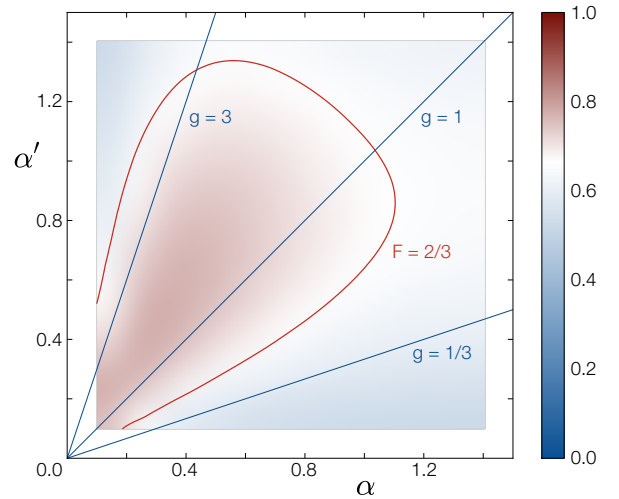


FIG. 3: Simulated average qubit teleportation fidelity as a function of input ( $\alpha$ ) and output state ( $\alpha'$ ) amplitudes. All relevant practical imperfections in our experimental setup, as described in the Supplementary Information, are taken into account. The red curve labelled “ $F = 2/3$ ” indicates the classical teleportation bound.

## Methods

**Experiment** We generated the squeezed vacua at 860 nm wavelength from an OPO (optical parametric oscillator) continuously pumped with pump parameters between 0.15 and 0.31, corresponding to  $\beta$  values of 0.78 to 1.15. We tapped off 5% of the squeezed beam on a BS and guided it to an APD. A click of the APD heralded the subtraction of a photon from the main beam<sup>15,27</sup>. The state thus generated is a close approximation to the odd cat state  $|\Phi_{-}\rangle$ , and has been shown to provide near-perfect teleportation performance<sup>31</sup>.

Whenever Alice’s APD clicked simultaneously with the heralding signal of the single-photon subtraction for the resource cat-state generation, the tele-amplification was successful, and we recorded a trace of the homodyne signal of Bob’s output state. The success probability is given by the ratio of the simultaneous click rate ( $\sim 3\text{--}28\text{ s}^{-1}$ ) to the photon subtraction click rate ( $\sim 1000\text{--}4500\text{ s}^{-1}$ ). It is mainly limited by detector and spectral filtering efficiency. To build the homodyne tomogram, we repeated this procedure 6000–24000 times for each fixed input state, with the local oscillator of the homodyne detector locked at phases  $-180^{\circ}, -150^{\circ}, \dots, 150^{\circ}$  with respect to the input state. Note that the protocol succeeds as a single shot for an unknown input state – the repeated measurements with identical inputs are only needed for characterizing the process by homodyne tomography.

Alice’s input states were independently characterized by homodyne tomography at port C by setting  $R_A = 1$ . To determine the input states accurately just at Alice’s BS, we correct their reconstruction for the detection efficiency and the propagation losses from that point to

the homodyne detector. This total efficiency amounts to 88%. Likewise, in the reconstruction of Bob's output states we correct for the overall detection efficiency of 94% but not for any propagation losses.

A more detailed description of the experimental setup and the state characterization can be found in the Supplementary Information.

**Simulation of cat-state qubit teleportation** A cat-state qubit can be represented on a Bloch sphere as

$$\begin{aligned} |\psi(\alpha, \theta, \phi)\rangle &= c_+ |\alpha\rangle + c_- |-\alpha\rangle \\ &= \cos\frac{\theta}{2} |\Phi_+(\alpha)\rangle + e^{i\phi} \sin\frac{\theta}{2} |\Phi_-(\alpha)\rangle, \end{aligned}$$

where  $|\Phi_{\pm}(\alpha)\rangle = \mathcal{N}_{\pm}(|\alpha\rangle \pm |-\alpha\rangle)$  are the even/odd cat

states with  $\mathcal{N}_{\pm} = 1/\sqrt{2(1 \pm e^{-2\alpha^2})}$  and  $c_{\pm} = \mathcal{N}_+ \cos\frac{\theta}{2} \pm \mathcal{N}_- e^{i\phi} \sin\frac{\theta}{2}$ .

Given an input state  $|\psi(\alpha, \theta, \phi)\rangle$ , our model of the experiment, described in Supplementary Information, returns a teleported output state  $\hat{\rho}_{\alpha, \theta, \phi}$ . To quantify the performance of the qubit teleportation for specific settings of  $\alpha$  and  $\alpha' = g_{\text{tg}}\alpha$ , we calculate the average fidelity of the teleported state with the target state by integrating over the Bloch sphere:

$$\mathcal{F}_{\alpha \rightarrow \alpha'}^{\text{avg}} = \int d\phi d\theta \frac{\sin\theta}{4\pi} \langle \psi(\alpha', \theta, \phi) | \hat{\rho}_{\alpha, \theta, \phi} | \psi(\alpha', \theta, \phi) \rangle.$$

The results for a range of amplitude settings are plotted in Fig. 3.

- 
1. Cochrane, P. T., Milburn, G. J. & Munro, W. J. Macroscopically distinct quantum-superposition states as a bosonic code for amplitude damping. *Phys. Rev. A* **59**, 2631–2634 (1999).
  2. Jeong, H. & Kim, M. S. Efficient quantum computation using coherent states. *Phys. Rev. A* **65**, 042305 (2002).
  3. Ralph, T. C., Gilchrist, A., Milburn, G., Munro, W. J. & Glancy, S. Quantum computation with optical coherent states. *Phys. Rev. A* **68**, 042319 (2003).
  4. Jeong, H. & Ralph, T. C. Schrödinger cat states for quantum information processing. in Cerf, N. J., Leuchs G. & Polzik, E. S., eds., *Quantum Information with Continuous Variables of Atoms and Light*, Ch. 9 (Imperial College Press, 2007).
  5. Lund, A. P., Ralph, T. C. & Haselgrove, H. L. Fault-tolerant linear optical quantum computing with small-amplitude coherent states. *Phys. Rev. Lett.* **100**, 030503 (2008).
  6. Gerry, C., Benmoussa, A. & Campos, R. Nonlinear interferometer as a resource for maximally entangled photonic states: Application to interferometry. *Phys. Rev. A* **66**, 013804 (2002).
  7. Joo, J., Munro, W. J. & Spiller, T. Quantum metrology with entangled coherent states. *Phys. Rev. Lett.* **107**, 083601 (2011).
  8. Sangouard, N. *et al.* Quantum repeaters with entangled coherent states. *J. Opt. Soc. Am. B* **27**, A137–A145 (2010).
  9. Brask, J. B. *et al.* Hybrid long-distance entanglement distribution protocol. *Phys. Rev. Lett.* **105**, 160501 (2010).
  10. Giovannetti, V. *et al.* Classical capacity of the lossy bosonic channel: The exact solution. *Phys. Rev. Lett.* **92**, 027902 (2004).
  11. Sasaki, M., Sasaki-Usuda, T., Izutsu, M. & Hirota, O. Realization of a collective decoding of code-word states. *Phys. Rev. A* **58**, 159–164 (1998).
  12. Waseda, A., Takeoka, M., Sasaki, M., Fujiwara, M. & Tanaka, H. Quantum detection of wavelength-division-multiplexing optical coherent signals. *J. Opt. Soc. Am. B* **27**, 259–265 (2010).
  13. Ourjoumtsev, A., Tualle-Brouiri, R., Laurat, J. & Grangier, P. Generating optical Schrödinger kittens for quantum information processing. *Science* **312**, 83–86 (2006).
  14. Neergaard-Nielsen, J. S., Nielsen, B. M., Hettich, C., Mølmer, K. & Polzik, E. S. Generation of a superposition of odd photon number states for quantum information networks. *Phys. Rev. Lett.* **97**, 083604 (2006).
  15. Wakui, K., Takahashi, H., Furusawa, A. & Sasaki, M. Photon subtracted squeezed states generated with periodically poled KTiOPO<sub>4</sub>. *Opt. Express* **15**, 3568–3574 (2007).
  16. Ourjoumtsev, A., Jeong, H., Tualle-Brouiri, R. & Grangier, P. Generation of optical 'Schrödinger cats' from photon number states. *Nature* **448**, 784–786 (2007).
  17. Takahashi, H. *et al.* Generation of large-amplitude coherent-state superposition via ancilla-assisted photon subtraction. *Phys. Rev. Lett.* **101**, 233605 (2008).
  18. Neergaard-Nielsen, J. S. *et al.* Optical continuous-variable qubit. *Phys. Rev. Lett.* **105**, 053602 (2010).
  19. Lee, N. *et al.* Teleportation of nonclassical wave packets of light. *Science* **332**, 330–333 (2011).
  20. van Enk, S. J. & Hirota, O. Entangled coherent states: Teleportation and decoherence. *Phys. Rev. A* **64**, 022313 (2001).
  21. Jeong, H., Kim, M. & Lee, J. Quantum-information processing for a coherent superposition state via a mixed entangled coherent channel. *Phys. Rev. A* **64**, 052308 (2001).
  22. Jacobs, B., Pittman, T. & Franson, J. Quantum relays and noise suppression using linear optics. *Phys. Rev. A* **66**, 052307 (2002).
  23. Collins, D., Gisin, N. & De Riedmatten, H. Quantum relays for long distance quantum cryptography. *J. Mod. Opt.* **52**, 735–753 (2005).
  24. Koashi, M. Unconditional security of coherent-state quantum key distribution with a strong phase-reference pulse. *Phys. Rev. Lett.* **93**, 120501 (2004).
  25. Tamaki, K., Lütkenhaus, N., Koashi, M. & Batuwantudawe, J. Unconditional security of the Bennett 1992 quantum-key-distribution scheme with a strong reference pulse. *Phys. Rev. A* **80**, 032302 (2009).
  26. Lo, H.-K. & Preskill, J. Security of quantum key distribution using weak coherent states with nonrandom phases. *Quant. Inf. Comp.* **7**, 431–458 (2007).
  27. Takeoka, M. *et al.* Engineering of optical continuous-variable qubits via displaced photon subtraction: mul-

- timode analysis. *J. Mod. Opt.* **58**, 266–275 (2011).
28. Xiang, G. Y., Ralph, T. C., Lund, A. P., Walk, N. & Pryde, G. J. Heralded noiseless linear amplification and distillation of entanglement. *Nature Photon.* **4**, 316–319 (2010).
  29. Zavatta, A., Fiurášek, J. & Bellini, M. A high-fidelity noiseless amplifier for quantum light states. *Nature Photon.* **5**, 52–60 (2010).
  30. Ferreyrol, F., Blandino, R., Barbieri, M., Tualle-Brouri, R. & Grangier, P. Experimental realization of a nondeterministic optical noiseless amplifier. *Phys. Rev. A* **83**, 063801 (2011).
  31. Brańczyk, A. & Ralph, T. C. Teleportation using squeezed single photons. *Phys. Rev. A* **78**, 052304 (2008).

*Acknowledgments* We acknowledge helpful discussions with K. Wakui, M. Takeoka, K. Hayasaka, M. Fu-

jiwara, T. C. Ralph, A. P. Lund, K. Tamaki, and M. Koashi. This work was partly supported by the Quantum Information Processing Project in the Program for World-Leading Innovation Research and Development on Science and Technology (FIRST) and by a National Research Foundation of Korea (NRF) grant funded by the Korean Government (Ministry of Education, Science, and Technology) (No. 2010-0018295).

*Author contributions* M.S. and J.S.N-N. formulated the basic protocol of tele-amplification and loss-tolerant quantum relay, inspired by a teleportation scheme by C.-W.L. and H.J.. J.S.N-N. and Y.E. carried out the experiment. J.S.N-N., C.-W.L., M.S. and H.J. performed the theoretical calculations. J.S.N-N. and M.S. wrote the paper with discussions and input from all the authors.